Simple Universal Kelvin Equation Valid in Critical Point Vicinity, External-Internal State Correction, and their Application in Argon Capillary Condensation in Mesoporous Silica MCM-41

A A Valeev[1], **E V Morozova**[1, 2]

[1] Kamyshin Technological Institute (branch) of Volgograd State Technical University, 6a, Lenina Street, Kamyshin, Volgograd Region, 403874, Russia
[2] Saint Petersburg Electrotechnical University "LETI", 5, Professora Popova Street, 197376, Russia

E-mail: antonvaleev@gmail.com

Abstract. A new simple universal form of the Kelvin equation, which can be used near the gas-liquid phase transition critical point, and the correction of the pressure and density for gas phase fluid outside the porous medium are taken into account for the argon meniscus effective curvature radius calculation at the phase equilibrium in mesoporous silica MCM-41 on the basis of the capillary condensation experimental data.

1. Introduction

Many methods for studying adsorption and condensation processes in porous media have been developed: traditional techniques (see the review paper [1]), CARS spectroscopy [2], NMR study [3], and positron annihilation spectroscopy [4]. We choose the works [5, 6] that have the relevant data for argon.

The model used in this work has already been applied to the two substances: CO_2 [7] and N_2 [8, 9]. In this work it will be applied to argon, which as well as nitrogen is used as a test medium to characterize the porosity. MCM-41 is a glass with a highly ordered structure, the pores being almost the same size. The model consists of the 2 main parts: the new Kelvin equation and the state transformation of the gas phase from inside the pores to the bulk. Section 2 will briefly show the new universal Kelvin equation that is also applicable near the critical point. Section 3 will shows the transformation of the gas phase state from the center of the hemispherical meniscus to the bulk. Bringing the two parts of the model together allows [7, 8, 9] one to get the gas-phase pressure outside the porous medium as a function of the meniscus effective curvature radius at the phase equilibrium inside the pores. Vice versa, one can find the radius as a function of the pressure in bulk. The latter is available in [5, 6] for several pore radii and temperatures. The results will be presented in section 4.

2. Simple universal Kelvin equation

In the work [7] a simple universal form of the Kelvin equation was deduced. The equation has two integral forms:

$$\int_{p_{sat}}^{\tilde{p}_{sat}} \frac{\rho_L - \rho_G}{\rho_G} dp_G = -2\sigma / r\,, \tag{1}$$

$$\int_{p_{sat}}^{\tilde{p}_{sat}^L} \frac{\rho_G - \rho_L}{\rho_L} dp_L = 2\sigma / r\,. \tag{2}$$

Here $\tilde{p}_{sat}^L$ is the pressure of the liquid phase in equilibrium with the saturated vapor at pressure $\tilde{p}_{sat}$ (one separated from another by the curved meniscus), p_{sat} is the saturated pressure in bulk, ρ_G, ρ_L and p_G, p_L are the phases' densities and pressures, respectively, σ is the surface tension, r is the effective curvature radius.

In order to take into account surface tension dependency on ρ_L and ρ_G, the parachor equation for pure fluids may be used [10]:

$$\sigma(T) = \left\{\wp(\rho_L(T) - \rho_G(T))\right\}^4, \tag{3}$$

where $\wp$ is the parachor of the fluid. In this equation, σ may be treated curvature independent, if the curvature radius is significantly greater than the Tolman's length [11]. More over, the authors of [12] stress that the equation (3) automatically accounts for the curvature, the latter manifesting itself through the change in density difference between the phases.

3. Internal chemical potential correction

The gas in the porous medium is attracted by the adsorbate and condensate molecules and also by the atoms of the porous medium. In this paper, the interaction with the porous medium is not taken into account. It can be reasonable if the adsorbate layer is thick enough. The good side of doing so is that the model can be used even when the pore radius is not known. The chemical potential of the gas phase in the presence of the force field can be split in two parts, the field one and the state one. The total chemical potential should remain the same inside and outside the porous medium. Thus one can put the equation [7-9]:

$$\mu_f' + \mu'(\rho', T) = \mu_f + \mu(\rho, T), \tag{4}$$

where $\mu_f' = 0$ and $\mu'(\rho', T)$ are the field and the state chemical potentials far outside the pores, μ_f and $\mu(\rho, T)$ are the ones inside the pores near the curved meniscus. Now we can put [7,8]:

$$\mu(\rho, T) - \mu'(\rho', T) = -\mu_f\,. \tag{5}$$

This equation shows the difference between the states inside and outside the porous medium.

$-\mu_f$ being positive reaches its approximate minimum in the center of the meniscus hemisphere. In this paper, will be considered minimal (not exact) μ_f. Thus the minimal necessary correction will be performed.

To proceed further, it is assumed that the liquid-like layer surrounding (at the moment of the condensation) the center of the meniscus hemisphere is composed [7] of the spherically organized fluid at one side and the cylindrically organized fluid at another side:

$$\mu_f = \frac{\mu_{f,sph} + \mu_{f,cyl}}{2}\,. \tag{6}$$

The expressions [7, 8] for them:

$$\mu_{f,sph} = -16\pi(n_L - n_V)N_A^2\varepsilon_{LL}\sigma_{LL}^6 \int_{r+\sigma/2}^{\infty} r^{-4} dr = -\frac{16\pi(n_L - n_V)N_A^2\varepsilon_{LL}\sigma_{LL}^6}{3(r + \sigma_{LL}/2)^3}, \tag{7}$$

$$\mu_{f,cyl} = -4\pi(n_L - n_V)N_A^2\varepsilon_{LL}\sigma_{LL}^6 \int_{-\infty}^{\infty}\int_{r+\sigma/2}^{\infty} (r^2 + z^2)^{-3} 2r dr dz = -\frac{\pi^2(n_L - n_V)N_A^2\varepsilon_{LL}\sigma_{LL}^6}{(r + \sigma_{LL}/2)^3}, \tag{8}$$

where $\mu_{f,sph}, \mu_{f,cyl}$ — the field chemical potentials due to interaction with the spherical and the cylindrical liquid surroundings, respectively, (N_A is the Avogadro number, n_L, n_V are liquid and vapor

phases molar concentrations, respectively; ε_{LL} and σ_{LL} are the fluid-fluid Lennard-Jones interaction parameters), $r+\sigma_{LL}/2$ is used instead of *r*, to account for the liquid molecule center shift from the phase separation surface. One may notice that in the integrals for $\mu_{f,sph}, \mu_{f,cyl}$, upper limits are set to ∞. This can be justified if the adsorbate is sufficiently thick. This equation corrects [8, 9] the analogous one of [7] by means of replacing n_L with $n_L - n_V$.

Now, in terms of the saturated pressure, equation (5) can be rewritten [7]:

$$\int_{\tilde{p}'_{sat}}^{\tilde{p}_{sat}} v_G dp_G = -\mu_f \,, \tag{9}$$

where $\tilde{p}'_{sat}$ is the pressure of vapor outside the porous medium in equilibrium with confined saturated vapor.

Both μ_f and $\tilde{p}_{sat}$ are functionally dependent on *r*. Thus $\tilde{p}'_{sat}$ is a function of *r*. Vice versa, *r* can be treated as a function of $\tilde{p}'_{sat}$. Consequently, if one knows the experimentally determined pressure $\tilde{p}'_{sat}$ [5, 6], one can estimate [7-9] the meniscus effective curvature radius as well.

In the next section, we apply the model to capillary evaporation/condensation of argon in MCM-41.

4. Calculating phase equilibrium as a function of the meniscus curvature

Argon is a nonpolar fluid. Thus its Tolman's length should be smaller than the molecule average diameter in the cases considered in this work.

The value 54.00 $dn^{1/4}cm^{11/4}/mol$ of [12] is used for the Ar parachor. For the Lennard-Jones potential, the authors will use the parameters [13] $\varepsilon_{LL} = 1.67\cdot10^{-21}$ J, $\sigma_{LL} = 0.340$ nm.

PC-SAFT EOS used in the work [12] behaves correctly in the instability region and therefore is suitable for handling the 'light phase'. In the present work, the treatment is limited to stability and metastability regions. Thus the choice of the EOS can be extended to high-accuracy empirical ones. The equation of state and the phase equilibrium equations of [14] will be chosen further on in this paper. For comparison the equation of state of [15] will be also used.

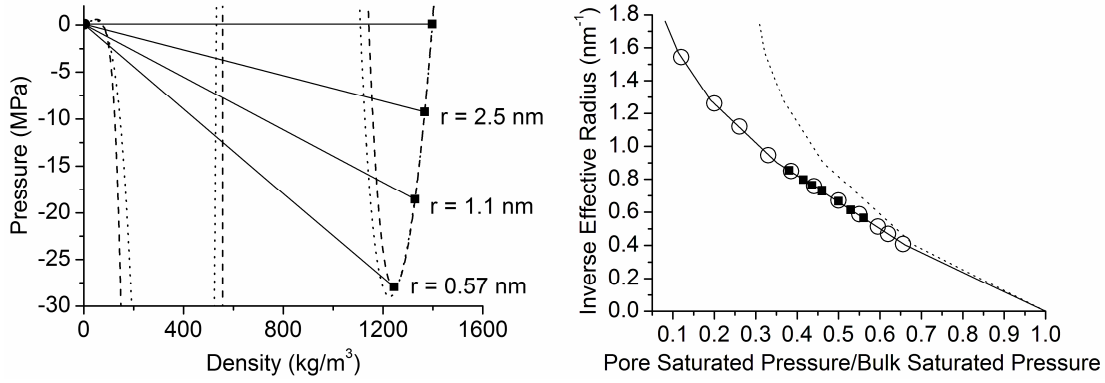

a b

Figure 1. Calculated phase equilibriums of Ar as a function of the spherical meniscus curvature radius for T = 87 K.

Using the integral equations (1), (2), the equations of state and the parachor equation (3), the phase equilibriums have been calculated. Pressure outside the pores is calculated using equation (9). In figure 1 - the calculated phase equilibriums of argon as a function of the spherical meniscus curvature radius for T = 87 K. In figure 1a the solid lines show some of the equilibriums. Horizontal line shows the phase equilibrium of the bulk argon. The dash and dot curves show the isotherms of [14] and [15], respectively, the former is used for calculations for its better accuracy. One may notice their similarity in stability and metastability regions. This fact supports the equations of state validity in the both regions. In figure 1b the dot and the solid curves show the inverse curvature radius as a function of

$\tilde{p}_{sat} / p_{sat}$ and $\tilde{p}'_{sat} / p_{sat}$, respectively. Now that we know the measured capillary condensation pressure [6], we are able to estimate the spherical meniscus effective curvature radius. To do so, the closed square and open round symbols may be put on the $\tilde{p}'_{sat} / p_{sat}$ curve accordingly with the experimental results [6] for the evaporation and condensation, respectively. As it has not been established [12,16-24] yet which (if either) of these processes takes place in the state of the thermodynamic equilibrium, the method suggested in this work is applied formally to the both of them, giving the possible inverse meniscus radii at the moment of the capillary evaporation and condensation. For the cases, in which the hysteresis is not observed, the open round symbols are used. The results are summarized in figure 2. There are shown the effective meniscus curvature radii at the capillary evaporation (closed symbols) and the condensation (open symbols) as a function of the sample pore radius. As soon as we know the latter, we are able to calculate the λ-parameter [12] as well (see figure 3). Figure 3 also shows partially the fit by a curve made in [12]. It should be mentioned that the results presented here are made with high-accuracy numerical methods. Figure 1 and the actions associated with it are used for the illustration purposes. The results of another work [5], dealing with the same sample at different temperatures, have passed the similar procedure. In figure 4 there are the effective meniscus curvature radii at the capillary evaporation (closed symbols) and the condensation (open symbols) as a function of the temperature. The λ-parameter is shown in figure 5 by rhombi. Analogous results for argon of [12] are shown by closed squares. In figure 5 rounds and open squares show the results for N_2 of [8] (recalculated [9] with a high-accuracy numerical scheme) and [12], respectively. Closed rounds show the results from the desorption branch. Triangles and stars show the results of the work [7] and the work [12], respectively. Open triangles show the results published in [7], where the capillary condensation pressures were taken indirectly from figure 3 of [5]. Closed triangles show the 'improved' results, where the capillary condensation pressure data were taken from figure 4 of [5], and also the corrected [8] equations (7), (8) were used.

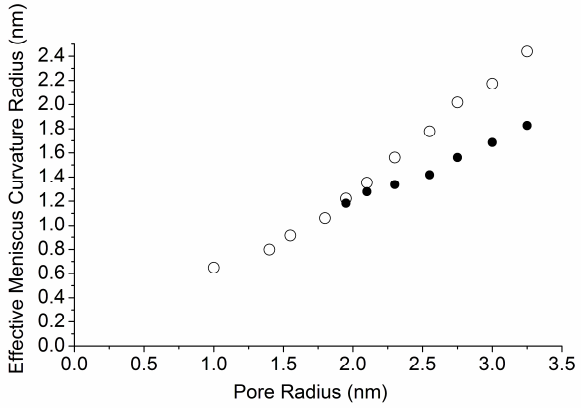

Figure 2. Effective meniscus curvature radii at the capillary evaporation (closed symbols) and condensation (open symbols) as a function of the sample pore radius at T = 87 K.

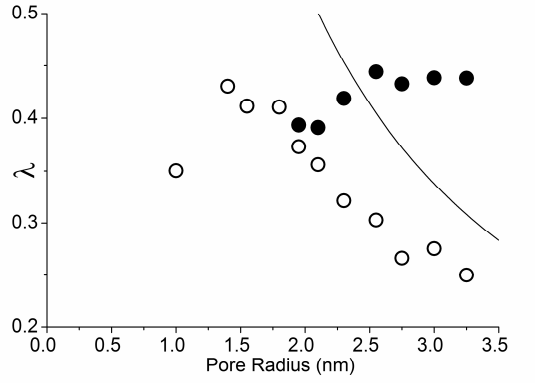

Figure 3. λ-parameter as a function of the pore radius at T = 87 K.

5. Conclusion

On the basis of the available capillary condensation data [5, 6], the spherical meniscus effective curvature radius at the moment of argon capillary condensation/evaporation in MCM-41 and the λ-parameter have been calculated for several pore radii and temperatures. On the basis of the results presented in this work and in the works [7, 8, 9] (in contrast to those of [12]), it can be concluded that the λ-parameter shows similar value in a wide range of the pore radii and temperatures, especially for the evaporation. The method used in this work is analogous to that used in [12] with the two most important exceptions. Firstly, instead of the 'light phase' the liquid phase is used. Secondly, the fact that the vapor state inside the pores differs from that in bulk is taken into account.

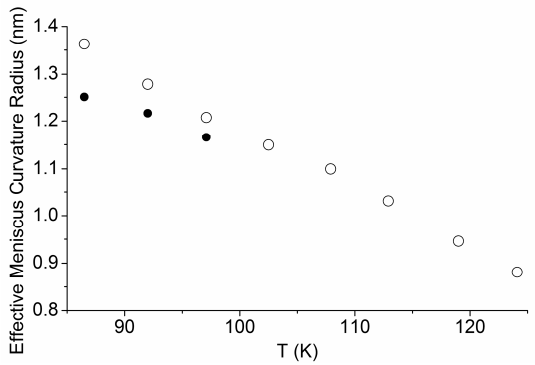

Figure 4. Spherical meniscus effective curvature radius at the moment of argon capillary condensation in MCM-41 as a function of the temperature.

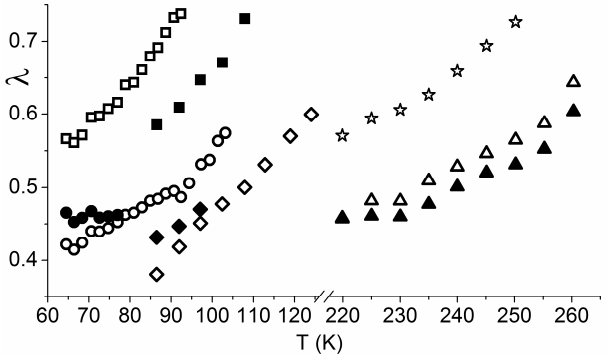

Figure 5. λ-parameter as a function of the temperature.

References

[1] Barsotti E, Tan S P, Saraji S, Piri M and Chen J-H 2016 *Fuel* **184** 344–361
[2] Arakcheev V G, Bekin A N and Morozov V B 2017 *Laser Phys.* **27** 115701
[3] Omi H, Nagasaka B, Miyakubo K, Ueda T and Eguchi T 2004 *Phys. Chem. Chem. Phys.* **6** 1299–1303
[4] Alam M A, Clarke A P and Duffy J A 2000 *Langmuir* **16** 7551–3
[5] Morishige K and Nakamura Y 2004 *Langmuir* **20** 4503–6
[6] Kruk M and Jaroniec M 2000 *Chem. Mater.* **12** 222–230
[7] Valeev A A and Morozova E V 2017 *Solid State Phenomena* **265** 392–397
[8] Valeev A A, Simple universal Kelvin equation valid in the critical point vicinity, external-internal state correction, and their application to nitrogen capillary condensation in mesoporous silica MCM-41: to be published
[9] Valeev A A and Morozova E V, Simple universal Kelvin equation valid in the critical point vicinity, external-internal state correction, and their application to nitrogen capillary condensation in mesoporous silica SBA-15: to be published
[10] Poling B E, Prausnitz J M and O'Connell J P 2001 *The Properties of Gases and Liquids* (New York: McGraw-Hill)
[11] Tolman R C 1949 *J. Chem. Phys.* **17** 333–337
[12] Tan S P and Piri M 2015 *Fluid Phase Equilibr.* **393** 48–63
[13] McGaughey A J H and Kaviany M 2004 *Int. J. Heat Mass Transfer* **47** 1783–98
[14] Tegeler Ch, Span R and Wagner W 1999 *J. Phys. Chem. Ref. Data* **28** 779–850
[15] Span R and Wagner W 2003 *Int. J. Thermophys.* **24** 41–109
[16] Morishige K and Ito M 2002 *J. Chem. Phys.* **117** 8036–41
[17] Evans R, Marini Bettolo Marconi U and Tarazona P 1986 *J. Chem. Phys.* **84** 2376–99
[18] Evans R, Marini Bettolo Marconi U and Tarazona P 1986 *J. Chem. Soc. Faraday Trans.* **82** 1763–87
[19] Ravikovitch P I, Domhnail S C Ó, Neimark A V, Schüth F and Unger K K 1995 *Langmuir* **11** 4765–72
[20] Neimark A V, Ravikovitch P I and Vishnyakov A 2000 *Phys. Rev. E* **62** R1493–96
[21] Vishnyakov A and Neimark A V 2001 *J. Phys. Chem. B* **105** 7009–20
[22] Heffelfinger G S, van Swol F and Gubbins K E 1988 *J. Chem. Phys.* **89** 5202–05
[23] Marini Bettolo Marconi U and van Swol F 1989 *Phys. Rev. A* **39** 4109–16
[24] Papandopulu A, van Swol F and Marini Bettolo Marconi U 1992 *J. Chem. Phys.* **97** 6942–52